AI in Sustainable Energy and Environment

Journal homepage: aisesjournal.com

Vol. 1, No. 1, 2025
25-35

Performance Enhancement and Predictive Modelling of Sponge-Augmented Solar Still Using Ensemble Learning Techniques

Pankaj Dumka[1*], Nitesh Pandey[2], Dhananjay R. Mishra[1], Rohit Mishra[1], Rishika Chauhan[3]

1. Department of Mechanical Engineering, Jaypee University of Engineering and Technology, A.B. Road, Raghogarh-473226, Guna, Madhya Pradesh, India
2. Department of Computer Science and Engineering, Jaypee University of Engineering and Technology, A.B. Road, Raghogarh-473226, Guna, Madhya Pradesh, India.
3. Department of Electronics and Communication Engineering, Jaypee University of Engineering and Technology, A.B. Road, Raghogarh-473226, Guna, Madhya Pradesh, India.

Article Info

Received 31 July 2025

Received in Revised form 10 August 2025

Accepted 16 August 2025

Published online .....

DOI:

Keywords

Solar still

Artificial intelligence

Desalination

Sustainability

Sponges

Abstract

In this study, an attempt has been made to compare the performance of a conventional solar still (CSS) with a modified solar still (MSS) augmented with sponges. Two identical single-slope solar stills have been built for this purpose, with sponges placed in the basin area to enhance capillary action-induced storage capacity and water surface area. Outdoor experiments were conducted under real weather conditions at Raghogarh, Guna (24° 39′N, 77° 19′E), India, for a basin water mass of 40 kg. The experimental results demonstrated a noticeable boost in distillation and efficiency when the CSS was modified with sponges. The cumulative distillate yield of MSS was observed to be 16.38% higher than that of CSS. The presence of sponges improved the overall efficiency of the still by 16.39%, reaching 36.86% compared to 31.67% for CSS. Sponges contributed to an 18.31% increase in distillate yield during the daytime and a 9.78% increase during nighttime, indicating their effectiveness in improving heat retention and capillary-assisted evaporation. Furthermore, multiple machine learning models were evaluated for predicting the performance of solar stills. Among the tested models, XGBoost demonstrated superior accuracy with an R^2 value of 0.9693 and minimal standard deviation, highlighting its robustness and reliability. The results highlight that integrating sponges with a conventional solar still can significantly enhance its efficiency and productivity, making it a viable solution for improving freshwater production.

1. Introduction

Worldwide people are affected by the lack of drinkable water due to various climatic changes, rapid industrialization and overpopulation. Desalination has been one of the economical and environmentally friendly method for extracting freshwater from saltwater. It uses continuous solar energy to produce freshwater [1]. Traditional method such with multi-stage flash distillation and reverse osmosis are dependent on fossil fuel. This method utilizes freely available solar energy a sustainable alternative method to produce freshwater from renewable energy source. However, conventional solar still have some limitations like low distillate yield, heat absorption and water evaporation [2]. So, to overcome from these limitations, various types of sensible heat storage materials (SHSMs) are used to increase the heat absorb, to increase the overall effectiveness of the conventional solar still (CSS) [3]. In-depth study on various heat exchange mechanisms such as thermal energy storage and phase change material are reported by researchers and scientists [4, 5].

Toosi et al. [6] have experimentally studied the use of hybrid NPCM, PCM and a magnetic field in a stepped solar still. The have reported boost on production rate by up to 98%. Bhargva et al. [7] have reported 19% improved productivity of the

✉ *Corresponding author: p.dumka.ipec@gmail.com (P. Dumka)*

[Downloaded from aisesjournal.com on 2026-11-17]

modified solar still (MSS) when a bamboo cotton wick was placed over the rectangular fins in the still basin in comparison to regular still. Dumka et al. [8] have studied the performance of solar still augmented with saltwater bottles. They have reported 25% increment in the efficiency of MSS as compared to CSS. Incorporation of saltwater bottles as thermal energy storage reservoirs have notable reduction in the cost of production distillate significantly by 20%. Safari et al. [9] have provided an extensive and comparative assessment of thermochemical water splitting cycles. Permanent ferrite ring magnets have been added by Dumka et al. [10] to serve as a sensible heat pocket and lessen the surface tension of water. According to Farzi et al. [11] the performance of CSS is impacted by the ideal grain size distribution. They demonstrated greater productivity and thermal efficiency were achieved by the sand-containing treatment with an average grain size of 2.8 mm. Goshayeshi et al. [12] have researched more effective desalination system, which suggested daily freshwater output in solar stills is greatly increased by adding paraffin containing 0.5 mass percent graphene oxide to a semicircular absorber. Dumka et al. [13] examine the presence of glass bottles packed with sand has resulted in a 139.45% boost in overall internal efficiency and the modified solar still (MSS) has produced 21.32% more than conventional solar still (CSS). To improve cooling technology, Basiri et al. [14] determined optimal design parameters and developed empirical formulas for computing the average Nusselt number by examining the air-side thermal performance of rectangular plate heat sinks under coupled convection.

Hashemian and Noorpoor [15] have reported study on an environmental analysis of a solar/wind-powered multigeneration unit that produces hydrogen and ammonia using thermos-eco. Dumka et al. [16] investigated the efficiency of a CSS by adding JCBs (jute-covered plastic balls) to it. They have reported 32.76% increment in overall thermal efficiency of MSS. The application of honeycomb pads to enhance the distillate production from the solar still by increasing the evaporation surface through capillarity was investigated by Kumar et al. [17]. Furthermore, Dumka et al. [18] reported using heat localisation and capillary rise in jute to improve the CSS's performance by combining plexiglass and jute. By altering the basin water mass, Kabeel et al. [19] investigated the effect of jute fabric made with sand as thermal energy storage on a CSS's production. For the basin water mass of 20kg from CSS, they have recorded distillate output of 5.5 and 5.9 kg/m2, respectively, without and with jute cloth knotting and sensible heat storage materials. Dumka and Mishra [20] experimentally reported a notable increase in the mean thermal efficiency by 31.04% by using ultrasonic fogger in MSS. They have also reported that the MSS produced 9.89% lower per liter cost of freshwater water. Despite significant advancements there is still a critical gap in the use of energy storage strategies for boosting the performance of conventional solar stills.

An effective approach for simulating and predicting the performance of solar thermal systems, such as solar stills, is machine learning [23]. By providing precise and efficient predictions under various climatic and design circumstances, these data-driven models aid in overcoming the drawbacks of experimental techniques [24]. To forecast the hourly yield of a modified solar still enhanced with sponges, many regression methods were assessed in this work, including Support Vector Regression (SVR), Random Forest, Gradient Boosting, and XGBoost [25]. Extensive field testing is greatly reduced when machine learning is used into solar still research, facilitating quick optimization and design validation [26].

Although there is substantial amount of potential for improving the sustainability and economic viability of solar stills through the integration of sponge for thermal energy storage. Therefore, the present study assessed how the performance of solar still was affected using natural storage material (Lofa Sponge). Analysis and reporting of the experimental results from the outdoor experiments conducted in November and December of 2024 have been completed. Sponges have been found to significantly increase the distillate production and efficiency in Modified solar still as compared to conventional solar still. Also, to enable precise and quick predictions of solar still performance, machine learning integration minimises experimental expenses and time while maximising system efficiency in the actual world.

2. Experimental setup

The experimentation was conducted in JUET Guna, India (24° 39′N, 77° 19′E), in November and December 2024. To conduct this study, two identical, single slope conventional solar still (CSS) with a basin size 1m2 were installed using FRP material that was 5mm thick. Its upper and

[Downloaded from aisesjournal.com on 2026-11-17]

lower vertical sides are, respectively, 0.48 and 0.2 meters high. The interior surface of solar stills was painted black to improve solar energy absorption. The solar still has been covered with a 4 mm thick transparent iron glass at a 15.6° angle to the ground.

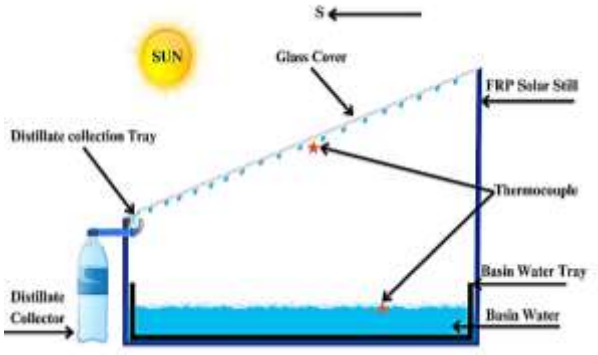


Figure 1. Diagrammatic representation of CSS.

Thirty-five sponges were compressed from cotton thread, measuring 13.2 cm average height and 3 cm average outer diameter. These sponges are coated with a thin coating of black fabric dye to improve its absorptivity of solar radiation. These sponges are used in the still for two reasons: first, they boost the surface are of the water by capillary action, which will improve the distillate output; second, they serve as natural energy storage in the still. The sponge-containing still is referred to as modified solar still (MSS). To maximize the floor area and prevent any sponge from interfering with one another, the sponges were positioned equally (Zigzag) apart inside the MSS basin tray. Figures 2 and 3 depict the layout of a sponges and the positioning of sponges in the tray, respectively.

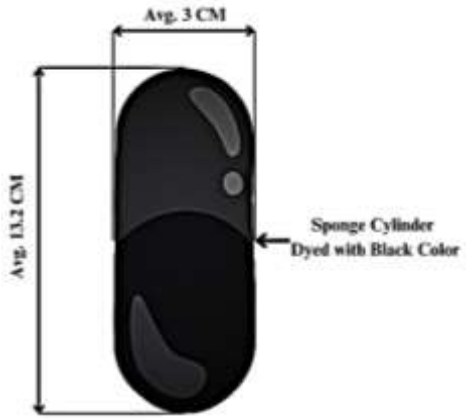


Figure 2. Diagrammatic of a sponge.

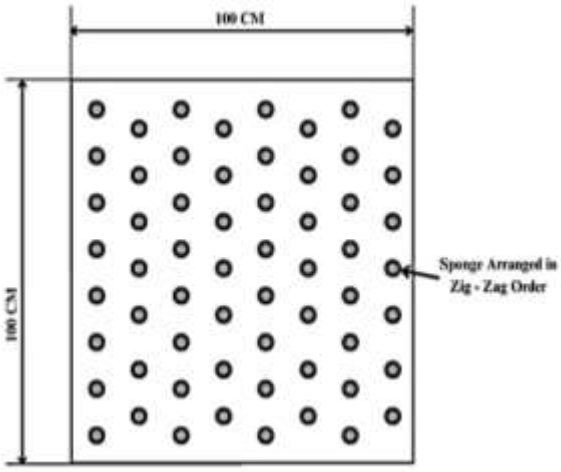


Figure 3. Arrangement of sponges in MSS

To measure the temperature of the atmosphere, inside and outside water, glass and basin, five K-type thermocouples (K 7/32-2C-TEF) were placed in the MSS as shown in Figure 4. Two more thermocouples were present to gauge the sponges inside and outside temperatures. A variety of temperatures were measured using a DTC324A-2 temperature indicator. During the experiment, an LX-107 solar power meter was used to detect incident sun radiation.

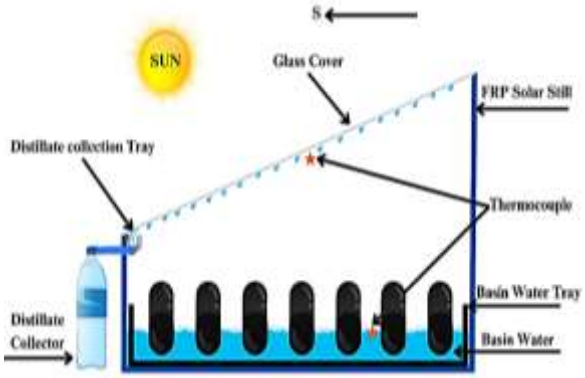


Figure 4. Diagrammatic representation of MSS.

Type B uncertainties are taken into consideration since it is expected that the data is distributed consistently among the experiment. This kind of standard uncertainty is assessed as [21]:

$$u = a/\sqrt{3} \quad (1)$$

Where a indicates the measuring device's accuracy. The standard uncertainty, range, and accuracy of the measurement devices are shown in Table 1.

Experiments were carried out un=sing two distinct basin water masses, namely 30 and 40 kg. Each experimental run lasts for 24 h. The field experiments yielded the following findings:

[Downloaded from aisesjournal.com on 2026-11-17]

- Temperature of the atmosphere, basin water, inside and outside glass, and sandbags.
- The amount of solar radiation that strikes an angled glass cover.
- The output of distillation is done every hour.

Table 1. Accuracy, range, and standard uncertainty of measuring instruments

Instrument	Accuracy	Range	Standard uncertainty
Graduated Cylinder	±1 ml	0 - 250 ml	0.6 ml
Thermocouple	±0.1ºC	-100 - 500ºC	0.06ºC
Solar Power meter	±10 W/m^2	0 - 1999 W/m^2	5.77 W/m^2

The solar overall efficiency of a solar still is defined as the ratio of the thermal energy required to generate a specific volume of distillate output to the total solar energy input. This may be stated mathematically as [22]:

$$\eta_{i=}\frac{\sum(\dot{m}_{ew}\times L)}{\sum(I(t)\times A_w\times L)}\times 100 \quad (2)$$

Where L is assessed by using the relation [10] and $T_v = (T_w + T_{ci})/2$.

3. Observation, results and disvussion

The amount of solar radiation that is incident and the surrounding temperature change throughout the duration of the day are shown in Figure 5. The intensity of solar radiation began at around 400 W/m² in the morning and peaked at 980 W/m² at around 13:00. By 18:00, it had progressively decreased to almost 0 W/m². the experiment, there were little changes in the ambient temperature. The graph shows how the intensity of solar radiation directly affects the thermal performance of the system.

Figure 6 shows the inner glass temperature (T_{ci}) and basin water temperature (T_w) change over time in CSS and MSS for a 40 kg basin water mass. Up until 15:00 hours, CSS's T_w is slightly higher than MSS's, after that, MSS overtakes CSS and holds a lead until the experiment's conclusion. This pattern results from the sponges in MSS having a greater capacity to retain heat, which aids in the progressive release and storage of heat over time. Similar trends have been seen in the inner glass temperature (T_{ci}), with CSS having a little higher T_{ci} than MSS in the early hours because of direct solar exposure. However, around 15:00 h, MSS overtakes CSS, demonstrating efficient heat retention and transmission inside the system. While T_{ci} hits 52.8°C in MSS and 54.3°C in CSS, the highest temperatures measured for basin water mass are 54.5°C for T_w in MSS and 56.1°C in CSS. The capillary rise-assisted evaporation from sponge surfaces in MSS is the primary cause of the minor difference in Tw between MSS and CSS, even though the T_w of MSS exceeds CSS after midday. However, MSS's effectiveness in long-term heat absorption and storage is highlighted by its capacity to hold and maintain greater temperatures in the latter hours.

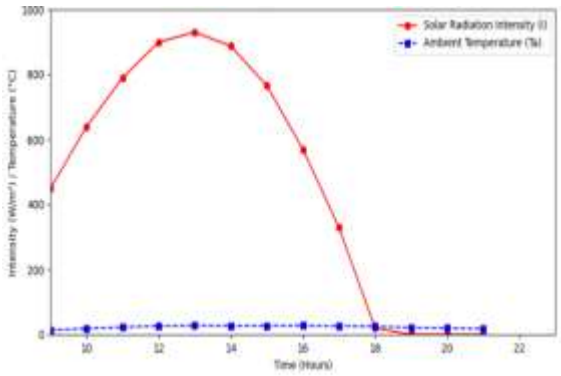


Figure 5. Solar radiation intensity and ambient temperature over time

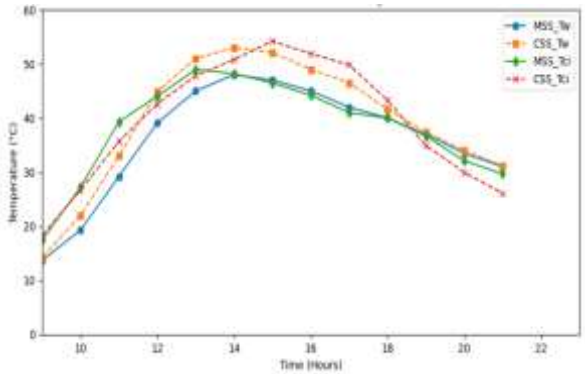


Figure 6. Basin water versus inner glass temperature.

The variation in MSS's sponge surface temperature (Tlofa) and basin water temperature (Tw) over time is depicted in Figure 7. Around 15:00, the highest recorded temperatures for Tlofa and T_w were 50.3°C and 51.7°C, respectively. At first, Tlofa closely tracks T_w, suggesting that the

[Downloaded from aisesjournal.com on 2026-11-17]

sponges are effectively absorbing heat. But after 15:00, Tlofa falls behind T_w, which is explained by the cooling impact caused by the sponge's faster rate of evaporation than that of the free water surface. By ensuring a steadier drop in temperature during the later hours of the experiment, this occurrence emphasises the function of sponges in controlling heat retention within the system.

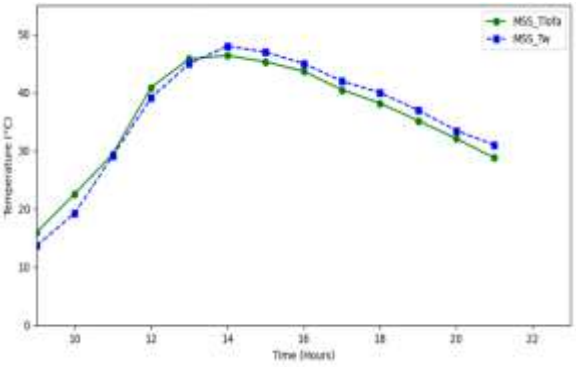


Figure 7. Sponge versus basin water temperature in MSS

Figure 8 demonstrates the hourly fluctuation of the distillate yield derived from MSS and CSS for the specified water mass. With a maximum production of 325 ml for MSS and 312 ml for CSS, respectively, MSS has a 4.17% higher yield. Because of the improved evaporation rate and perceptive energy storage in MSS, the overall yield reported from Modified CSS and CSS is 2.316 L and 1.99 L, respectively. This results in an overall improvement of 16.38% in cumulative distillate output. During the day (≤18 hours), the distillate yield improvement for MSS over CSS is 18.31%, while during the night (>18 hours), it is 9.78%. This enhanced nighttime production is a result of sponges' increased surface area, capillary rise, and energy storage capacity. These results imply that sponges greatly increase CSS's everyday output.

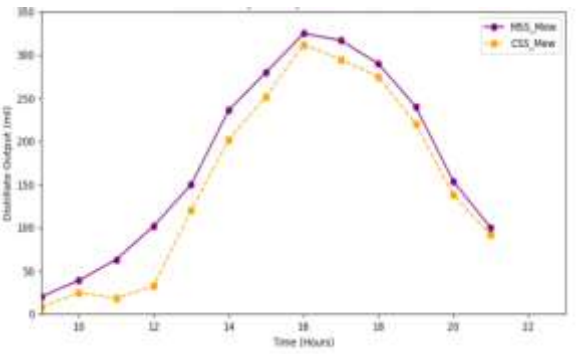


Figure 8. Distillate output comparison for MSS and CSS

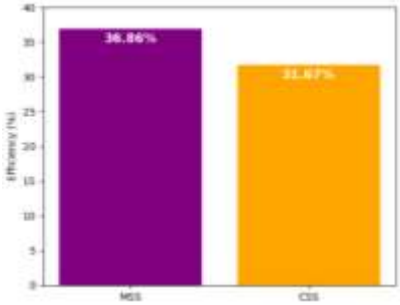


Figure 9. Overall efficiency of MSS and CSS

The total effectiveness of CSS and MSS is shown in Figure 9. For CSS and MSS, the corresponding efficiencies are 31.67% and 36.86%. The system's total efficiency has increased by 16.39% after the sponges were supplemented with CSS. MSS is now more efficient thanks to the strong capillary action-assisted evaporation from the sponges.

To further validate the results received form the experiment and for future predictions and analysis authors have tested the data by using different algorithms (e.g., linear regression, random forest, decision tree, support vector regressor and gradient boosting). This helps capture the complex thermal and physical behaviour involved in solar evaporation and condensation. Basic models like Linear Regression provide a starting point, but often fail to capture nonlinear relationships in solar still performance data. Tree-based models like Decision Tree and Random Forest are better at handling nonlinearity and feature interactions. They can model sudden changes in productivity due to varying sponge material or ambient conditions. Similarly, Support Vector Regressor (SVR) and Gradient Boosting Regressor (GBR) offer robustness and precision, especially in small or noisy datasets.

The correlation matrix presents high correlation between MSS and CSS due to similar parameters (e.g.,Tw, Tci), suggesting consisteny between the methods as shown in Figure 10. This matrix presents that the MSS_Tlofa shows a strong positive correlation with MSS_Mew which shows the strong potential as a strong predictor.

The boxplot clearly differentiates MSS_Mew and CSS_Mew shown in Figure 11, as the MSS is having lofa in it that why it is showing higher median and wider spread compared to CSS_Mew. This indicates that MSS consistently yields more evaporated water across varying conditions. The wider spread also suggests that MSS responds more dynamically to environmental changes, which is beneficial for optimization.

[Downloaded from aisesjournal.com on 2026-11-17]

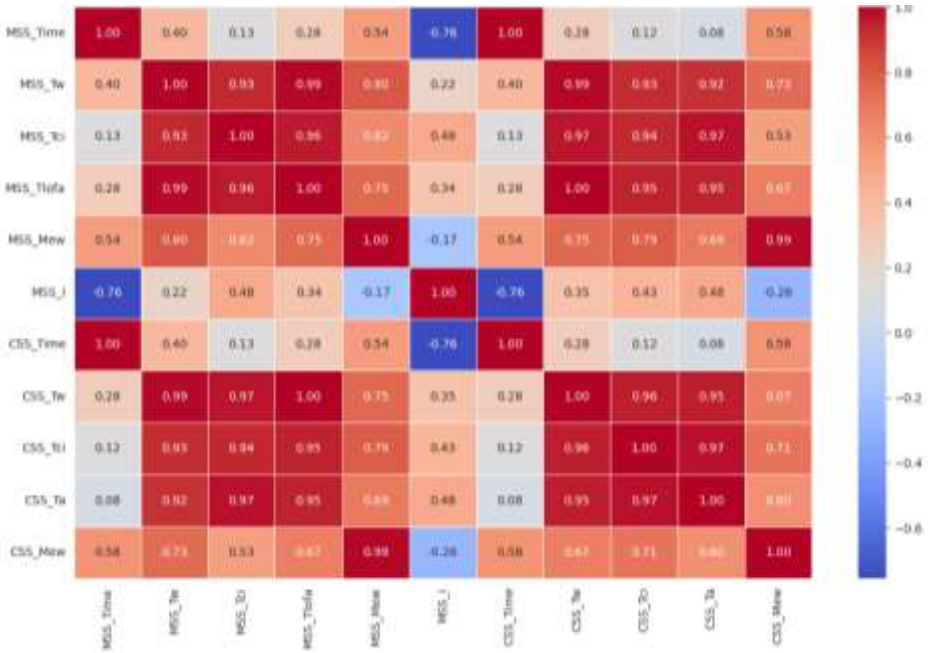


Figure 10. Correlation matrix – MSS and CSS

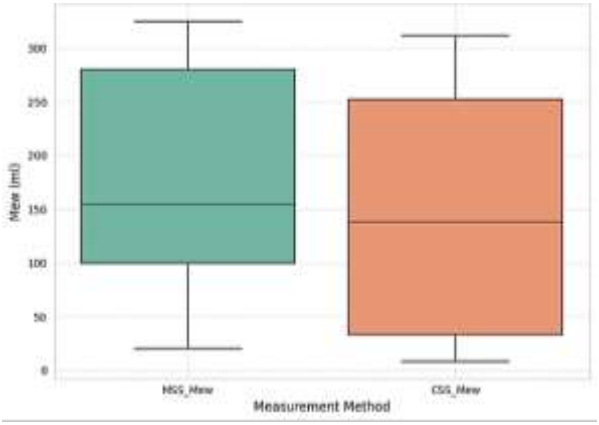


Figure 11. Comparison between MSS and CSS Methods

Figure 12 is the pairplot shows strong linear relationships between MSS_Mew and features like MSS_Tw, MSS_Tci, and MSS_Tlofa. These relationships suggest that as the temperature in the basin and surrounding surfaces increases, the amount of water evaporated also increases in a linear fashion, which is expected due to the enhanced evaporation at higher temperatures. MSS_I shows a less direct, possibly non-linear, relationship with MSS_Mew. This is since while solar irradiance drives the heating process, its effect on productivity is mediated through the temperature rise of water and other components, which might introduce some non-linearity or time lag in the response. Also, multicollinearity among the temperature features (MSS_Tw, MSS_Tci, MSS_Tlofa) is evident. This means these variables are highly correlated with each other—likely because they all respond similarly to solar input and heat transfer in the still.

The findings of the single split and cross-validation analyses of the Linear Regression model differ significantly as shown in Figure 13. With an MSE of 1843.917 and an R^2 of 0.848, the model exhibits good performance on a single train-test split, suggesting a strong fit. The model, however, shows very high error (Mean MSE: 44706.633) and a substantially negative R^2 (Mean R^2: -116.557) with large standard deviations during 5-fold cross-validation. This implies that the model may be extremely sensitive to data volatility and is not generalising well across various data splits.

Featuring a lower MSE of 1335.333 and a higher R^2 of 0.890, the adjusted Decision Tree model outperforms Linear Regression on a single train-test split, demonstrating significant predictive capabilities on the given split as shown in Figure 14. Cross-validation findings, however, suggest inconsistency: the model has a significant standard deviation and a higher Mean MSE of 11193.233 with a negative Mean R^2 of -12.840. These differences show that the model lacks generalisation over the entire dataset, even though it fits well to data subsets. Despite being more effective than linear models in capturing non-linear relationships, decision trees are less dependable without adequate regularisation due to a tendency to overfit.

[Downloaded from aisesjournal.com on 2026-11-17]

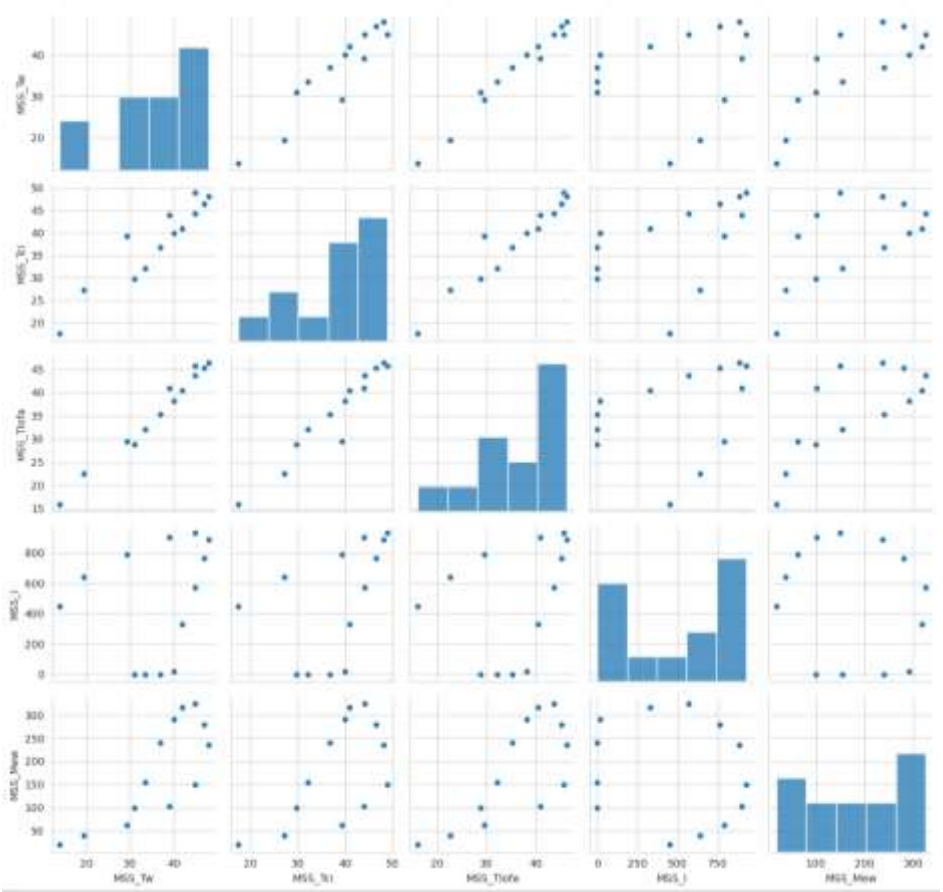


Figure 12. Pairplot of MSS features and target

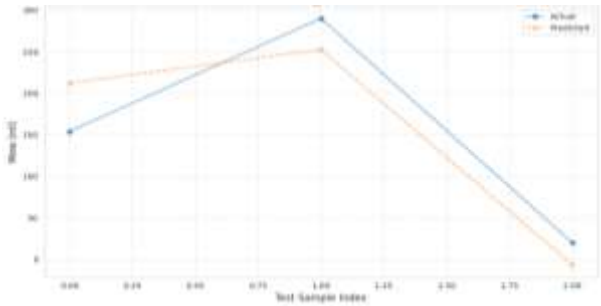


Figure 13. MSS_Mew Prediction using Linear Regression

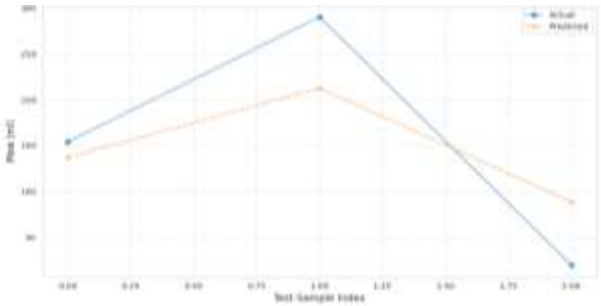


Figure 15. MSS_Mew Prediction using Random Forest

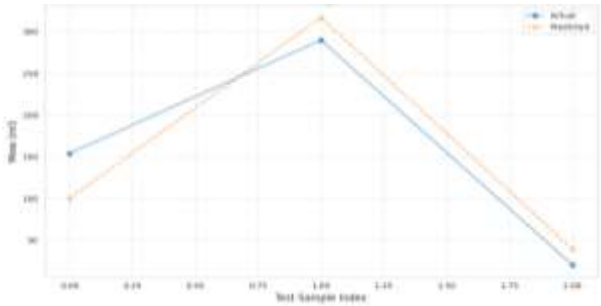


Figure 14. MSS_Mew Prediction using Decision Tree

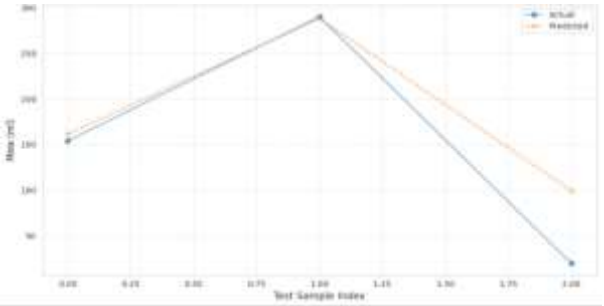


Figure 16. MSS_Mew Prediction using Support Vector Regressor

[Downloaded from aisesjournal.com on 2026-11-17]

Using 100 n_estimators and no depth limitation, the tweaked Random Forest model performs moderately on the single train-test split (MSE: 3668.564, R^2: 0.698), suggesting that it may account for a portion of the variation in MSS_Mew. The model's performance, however, drastically declines over 5-fold cross-validation, exhibiting a high Mean MSE of 10185.986, a negative Mean R^2 of -14.846, and a sizable standard deviation as shown in Figure 15.

With an MSE of 2123.261 and an R^2 of 0.825, the adjusted Support Vector Regressor (SVR), set up with C=100, gamma='auto', and a rbf kernel, performs well on the single train-test split, suggesting a strong fit to that subset. With a high Mean MSE of 8669.841 and a highly negative Mean R^2 of -19.617, together with a huge standard deviation, its performance drastically declines after 5-fold cross-validation as depicted in Figure 16.

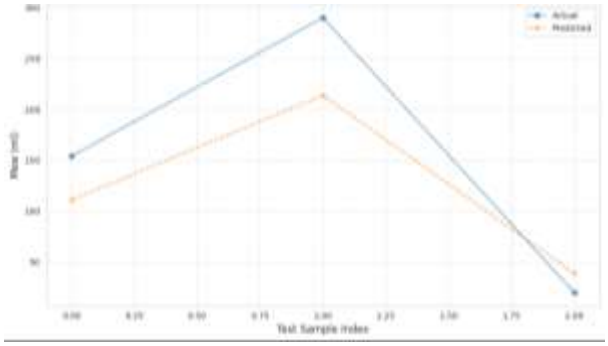


Figure 17. MSS_Mew Prediction using Gradient Boosting

Figure 17 shows a combination of an MSE of 2665.715 and R^2 of 0.781, the tuned Gradient Boosting Regressor, optimised with learning_rate=0.2, max_depth=3, and n_estimators=200, performs rather well on the single split evaluation. However, as demonstrated by a high Mean MSE of 10525.234 and a negative Mean R^2 of -13.450 with a huge standard deviation, its generalisation ability significantly decreases throughout 5-fold cross-validation. This notable decline implies that although the model successfully identifies patterns in a single split, it finds it difficult to remain consistent over different data splits.

When it came to predicting the output of the single slope solar still enhanced with sponges, the XGBoost model performed well as shown in Figure 18. With an R^2 score of 0.855 and an MSE of 1760.369 in the single train-test split, XGBoost was able to explain approximately 85.5% of the output variance with a comparatively low prediction error. Additionally, its 5-fold cross-validation findings indicate that it predicts more consistently across folds than other models, with the lowest standard deviations (MSE: 6959.529, R^2: 8.598) and a mean MSE of 8472.196 and mean R^2 of -10.191. Although the Decision Tree demonstrated a slightly superior R^2 in a single split (0.890), it had more variability in cross-validation. XGBoost provides a better balance between accuracy and generalization.

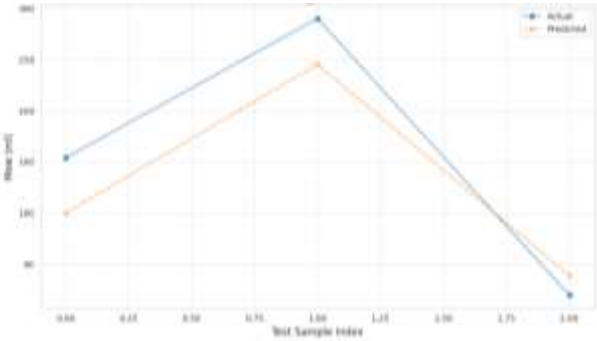


Figure 18. MSS_Mew Prediction using XGBoost

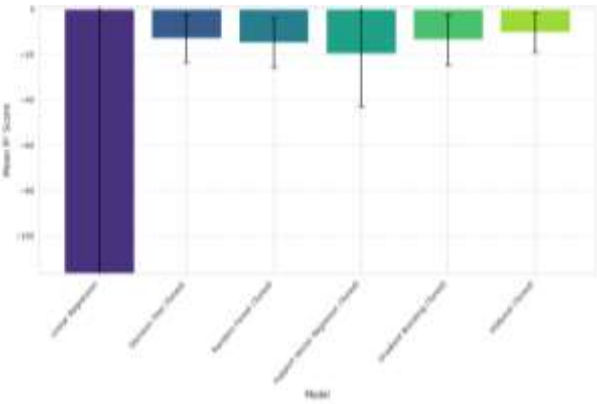


Figure 18. Model Comparison: Mean R^2 from 5-Fold Cross-Validation

The mean R^2 scores from 5-fold cross-validation are used in this bar chart to compare six machine learning models' performance as shown in Figure 18. The model's ability to explain the variance in the target variable (solar still output) is indicated by the R^2 value. Among advanced models, XGBoost (Tuned) has the shortest standard deviation and the least negative R^2 value, indicating reasonably solid and reliable predictions. On the other hand, linear regression exhibits poor generalisation, as seen by its extremely large standard deviation and severely negative mean R^2. This image demonstrates how the resilience and reduced variance of tree-based ensemble models, such as XGBoost and Gradient Boosting, make them more appropriate for this nonlinear dataset.

[Downloaded from aisesjournal.com on 2026-11-17]

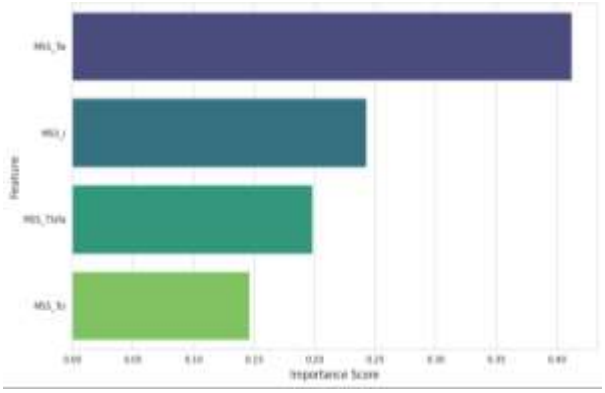


Figure 19. Feature Importance – Tuned Random Forest

The relative significance of each input feature in the XGBoost model is shown in this horizontal bar chart. The most significant predictor of the output of the solar still is MSS_Tw (water temperature in the basin), which is followed by solar intensity (MSS_I), sponge outlet temperature (MSS_Tlofa), and sponge inlet temperature (MSS_Tci). Since evaporation and, therefore, distillate output is directly impacted by water temperature, MSS_Tw's supremacy is consistent with thermal principles. This image is essential for directing engineering design since it shows where enhancements or sensor locations may maximise performance optimisation and forecast accuracy.

Table 2. Fold Cross-Validation – MSE (Mean & Std)

Model	Mean MSE	Std Dev	Rank
XGBoost (Tuned)	8472	6959	1st (Best)
SVR (Tuned)	8669	6854	2nd
Gradient Boosting	10525	8477	3rd
Random Forest	10185	6388	4th
Decision Tree (Tuned)	11193	8932	5th
Linear Regression	44706	57774	6th

Evaluating multiple models ensures that the most reliable one for predicting distilled water output under different environmental or design conditions. Cross-validation (5-fold) shows the models generalization beyond the training set, which is difficult for solar stills being tested under variable solar radiation and temperature profiles.

Table 3. Single train-test split (R^2 and MSE)

Model	MSE	R^2	Rank
Decision Tree (Tuned)	1335	0.890	1st (Best)
XGBoost (Tuned)	1760	0.855	2nd
Linear Regression	1843	0.848	3rd
SVR (Tuned)	2123	0.825	4th
Gradient Boosting	2665	0.781	5th
Random Forest	3668	0.698	6th

By analyzing both single split and cross-validation results as compared in table 3 & 4, the XGBoost model appears to be the most suitable for predicting solar still output. It shows a strong performance with a relatively low Mean Squared Error (MSE) of 8472.19 in cross-validation and the lowest standard deviation (6959.53) among all models, indicating consistent and reliable predictions as shown in table 2.

Table 4. 5-Fold Cross-Validation – R^2 score (Mean)

Model	Mean R^2	Std Dev	Rank
XGBoost (Tuned)	-10.19	8.59	1st (Least negative)
Decision Tree (Tuned)	-12.84	10.39	2nd
Gradient Boosting	-13.45	11.34	3rd
Random Forest	-14.85	11.03	4th
SVR (Tuned)	-19.61	23.33	5th
Linear Regression	-116.55	198.55	6th

Additionally, in the single train-test split, XGBoost achieved a high R^2 score of 0.855, highlighting its accuracy in capturing the underlying patterns in the data. In real-world applications, this approach reduces the dependency on time-consuming physical experiments. Once trained and validated, the model can efficiently predict solar still performance under different conditions, thereby saving significant time and operational costs.

4. Conclusion

Experimental evaluations of CSS and MSS's performance were conducted in a range of ambient temperature and sun radiation levels. The experiment evaluated both systems' distillate

[Downloaded from aisesjournal.com on 2026-11-17]

production, evaporation efficiency, and thermal behaviour over time. The experimental findings lead to the following deductions:

- The system's thermal performance was directly impacted by the solar radiation intensity, which peaked at 980 W/m² at around 13:00 and then steadily declined to almost 0 W/m² by 18:00.
- Although the sponges in MSS improved heat retention, the basin water temperature (Tw) in CSS was greater than that of MSS until 15:00. After that, MSS overtook CSS. For MSS and CSS, the highest Tw measured was 54.5°C and 56.1°C, respectively.
- A similar pattern was seen in the inner glass temperature (Tci), with CSS reaching 54.3°C and MSS 52.8°C. However, MSS shown improved long-term heat retention due to the sponges.
- Later in the experiment, the temperature dropped more gradually because the sponges in MSS were better at absorbing and storing heat. Due to increased evaporation from the sponge surface, the maximum measured sponge surface temperature (Tlofa) at 15:00 was 50.3°C, which was somewhat lower than Tw.
- With a maximum hourly output of 325 ml for MSS and 312 ml for CSS, distillate yield was greatly increased in MSS. With a cumulative output of 2.316 L for MSS and 1.99 L for CSS, the total improvement was 16.38%.
- Sponge storage and utilisation of stored heat energy is demonstrated by the 18.31% yield enhancement during the day (≤18 hours) and the 9.78% yield improvement during the night (>18 hours).
- Due to the capillary rise-assisted evaporation from the sponges in MSS, the overall system efficiency rose by 16.39% to 36.86% and 31.67% for CSS.
- The XGBoost (Tuned) model gave the best performance with an R^2 score of 0.9693 and standard deviation of 0.0217, showing excellent accuracy and consistency.
- The Gradient Boosting model achieved an R^2 of 0.9517 with standard deviation of 0.0245, performing close to XGBoost.
- The Random Forest model resulted in an R^2 of 0.9359 and a slightly higher standard deviation of 0.0368, indicating moderate consistency.
- The Support Vector Regressor (SVR) gave an R^2 of 0.9212 with standard deviation of 0.0341, maintaining stable but slightly lower predictive power.
- The Linear Regression model performed the worst with an R^2 score of -0.1804 and standard deviation of 0.1206, failing to model nonlinear behavior effectively.

5. References

[1]. Bacha, H. B., Joseph, A., Abdullah, A. S., & Sharshir, S. W. (2024). Synergizing water desalination and hydrogen production using solar stills with novel sensible heat storage and an alkaline electrolyzer. Case Studies in Thermal Engineering, 105663.

[2]. Anburaj, P., Vijayakumar, R., Kumar, R. V., Chanda, J., & Parvez, Y. A. (2025). Enhancing inclined solar still performance for effective desalination: A comparative study on combination of bamboo wick and metal energy storage materials. Solar Energy, 287, 113218.

[3]. Dhivagar, R., Shoeibi, S., Kargarsharifabad, H., Sadi, M., Arabkoohsar, A., & Khiadani, M. (2024). Performance analysis of solar desalination using crushed granite stone as an energy storage material and the integration of solar district heating. Energy Sources, Part A: Recovery, Utilization, and Environmental Effects, 46(1), 1370–1388. https://doi.org/10.1080/15567036.2023.2299693

[4]. Kabeel, A. E., Arunkumar, T., Denkenberger, D. C., & Sathyamurthy, R. (2017). Performance enhancement of solar still through efficient heat exchange mechanism–a review. Applied Thermal Engineering, 114, 815-836.

[5]. Panchal, H., & Mohan, I. (2017). Various methods applied to solar still for enhancement of distillate output. Desalination, 415, 76-89.

[6]. Toosi, S. S. A., Goshayeshi, H. R., Zahmatkesh, I., & Nejati, V. (2023). Experimental assessment of new designed stepped solar still with Fe3O4+ graphene oxide+ paraffin as nanofluid under constant magnetic field. Journal of Energy Storage, 62, 106795.

[7]. Bhargva, M., Sharma, M., Yadav, A., Batra, N. K., & Behl, R. K. (2023). Productivity augmentation of a solar still with rectangular fins and bamboo cotton wick. Journal of Solar Energy Research, 8(2), 1410-1416.

[8]. Dumka, P., Pandey, N., & Mishra, D. R. (2024). Conventional Solar Still Augmented with Saltwater Bottles: An Experimental Study. Journal of Solar Energy Research, 9(1), 1811-1821.

[9]. Safari, F., & Dincer, I. (2020). A review and

[Downloaded from aisesjournal.com on 2026-11-17]

comparative evaluation of thermochemical water splitting cycles for hydrogen production. Energy Conversion and Management, 205, 112182.

[10]. Dumka, P., Kushwah, Y., Sharma, A., & Mishra, D. R. (2019). Comparative analysis and experimental evaluation of single slope solar still augmented with permanent magnets and conventional solar still. Desalination, 459, 34-45.

[11]. Farzi, A., Nameni, R., & Asadollahi Yazdi, H. (2021). Enhancement of single slope solar still using sand: the effect of sand grain size distribution. Journal of Solar Energy Research, 6(2), 740-750.

[12]. Goshayeshi, H. R., Chaer, I., Yebiyo, M., & Öztop, H. F. (2022). Experimental investigation on semicircular, triangular and rectangular shaped absorber of solar still with nano-based PCM. Journal of Thermal Analysis and Calorimetry, 1-13.

[13]. Dumka, P., Gautam, H., Sharma, S., Gunawat, C., & Mishra, D. R. (2022). Impact of sand filled glass bottles on performance of conventional solar still. Journal of Basic & Applied Sciences, 18, 8-15.

[14]. Basırı, M., Goshayeshı, H. R., Chaer, I., Pourpasha, H., & Herıs, S. Z. (2023). Experimental study on heat transfer from rectangular fins in combined convection. Journal of Thermal Engineering, 9(6), 1632-1642.

[15]. Hashemian, N., & Noorpoor, A. (2023). Thermo-eco-environmental Investigation of a Newly Developed Solar/wind Powered Multi-Generation Plant with Hydrogen and Ammonia Production Options. Journal of Solar Energy Research, 8(4), 1728-1737.

[16]. Dumka, P., Chauhan, R., & Mishra, D. R. (2020). Experimental and theoretical evaluation of a conventional solar still augmented with jute covered plastic balls. Journal of Energy Storage, 32, 101874.

[17]. Kumar, R., Mishra, D. R., & Dumka, P. (2024). Improving solar still performance: A comparative analysis of conventional and honeycomb pad augmented solar stills. Solar Energy, 270, 112408.

[18]. Dumka, P., Mishra, D. R., Singh, B., Chauhan, R., Siddiqui, M. I. H., Natrayan, L., & Shah, M. A. (2024). Enhancing solar still performance with Plexiglas and jute cloth additions: experimental study. Sustainable Environment Research, 34(1), 3.

[19]. Kabeel, A. E., El-Agouz, S. A., Sathyamurthy, R., & Arunkumar, T. (2018). Augmenting the productivity of solar still using jute cloth knitted with sand heat energy storage. Desalination, 443, 122-129.

[20]. Dumka, P., & Mishra, D. R. (2020). Performance evaluation of single slope solar still augmented with the ultrasonic fogger. Energy, 190, 116398.

[21]. Esfahani, J. A., Rahbar, N., & Lavvaf, M. (2011). Utilization of thermoelectric cooling in a portable active solar still—an experimental study on winter days. Desalination, 269(1-3), 198-205.

[22]. Dumka, P., & Mishra, D. R. (2018). Energy and exergy analysis of conventional and modified solar still integrated with sand bed earth: Study of heat and mass transfer. Desalination, 437, 15-25.

[23]. Abdullah, A. S., Joseph, A., Kandeal, A. W., Alawee, W. H., Peng, G., Thakur, A. K., & Sharshir, S. W. (2024). Application of machine learning modeling in prediction of solar still performance: a comprehensive survey. Results in Engineering, 21, 101800.

[24]. Maddah, H. A., Bassyouni, M., Abdel-Aziz, M. H., Zoromba, M. S., & Al-Hossainy, A. F. (2020). Performance estimation of a mini-passive solar still via machine learning. Renewable Energy, 162, 489-503.

[25]. Wang, Y., Kandeal, A. W., Swidan, A., Sharshir, S. W., Abdelaziz, G. B., Halim, M. A., ... & Yang, N. (2021). Prediction of tubular solar still performance by machine learning integrated with Bayesian optimization algorithm. Applied Thermal Engineering, 184, 116233.

[26]. Gao, W., Shen, L., Sun, S., Peng, G., Shen, Z., Wang, Y., ... & Yang, N. (2023). Forecasting solar still performance from conventional weather data variation by machine learning method. Chinese Physics B, 32(4), 048801.

[Downloaded from aisesjournal.com on 2026-11-17]

[Downloaded from aisesjournal.com on 2026-11-17]